General Disclaimer

One or more of the Following Statements may affect this Document

- This document has been reproduced from the best copy furnished by the organizational source. It is being released in the interest of making available as much information as possible.

- This document may contain data, which exceeds the sheet parameters. It was furnished in this condition by the organizational source and is the best copy available.

- This document may contain tone-on-tone or color graphs, charts and/or pictures, which have been reproduced in black and white.

- This document is paginated as submitted by the original source.

- Portions of this document are not fully legible due to the historical nature of some of the material. However, it is the best reproduction available from the original submission.
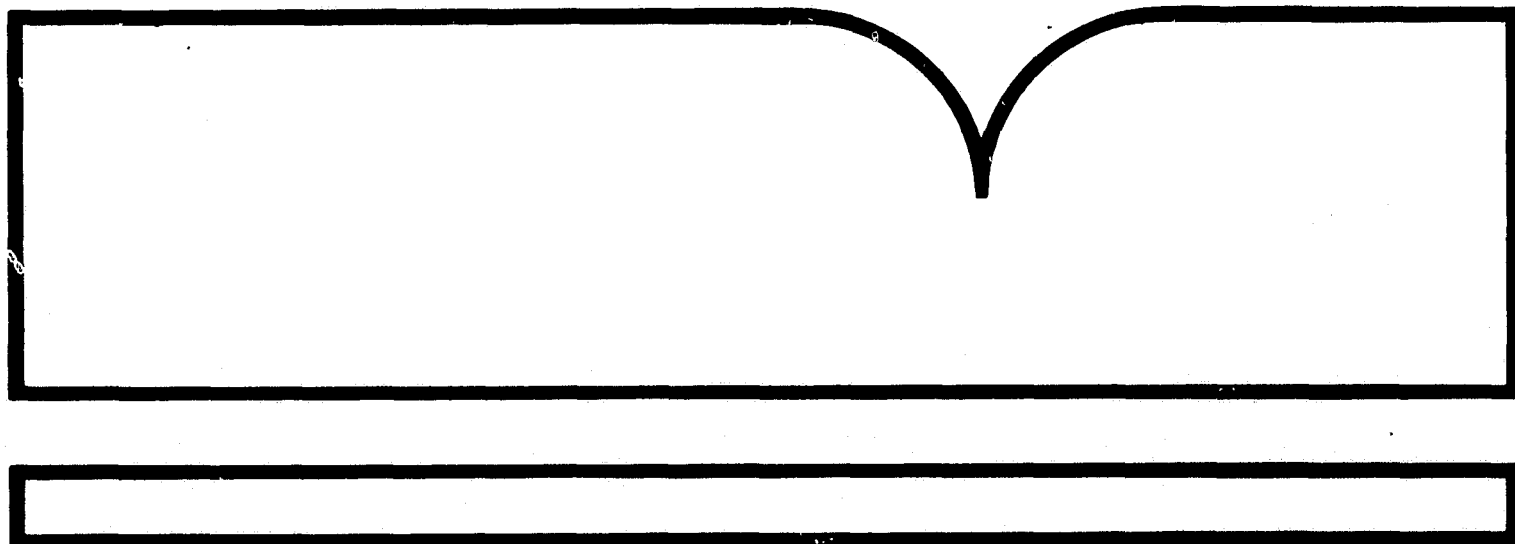
Semiconductor Technology
Program - Progress Briefs

(U.S.) National Bureau of Standards
Washington, DC

Prepared for

Defense Advanced Research Projects Agency
Arlington, VA

Nov 81

NBSIR 81-2230-3

Semiconductor Technology Program Progress Briefs

U.S. DEPARTMENT OF COMMERCE
National Bureau of Standards
National Engineering Laboratory
Center for Electronics and Electrical Engineering
Semiconductor Devices and Circuits Division
and
Semiconductor Materials and Processes Division

November 1981

SEMICONDUCTOR TECHNOLOGY PROGRAM

TABLE OF CONTENTS

ABSTRACT - This report provides information on the current status of NBS work on measurement technology for semiconductor materials, process control, and devices. Emphasis is placed on silicon and silicon-based devices. Highlighted activities include semi-insulating GaAs characterization, an automatic scanning spectroscopic ellipsometer, linewidth measurement and coherence, bandgap narrowing effects in silicon, the evaluation of electrical linewidth uniformity, and arsenic-implanted profiles in silicon. In addition, recent publications and publications in press are listed. The report is not meant to be exhaustive; contacts for obtaining further information are listed.

KEY WORDS - Electronics; integrated circuits; measurement technology; microelectronics; semiconductor devices; semiconductor materials; semiconductor process control; silicon.

Preface

This report covers results of work during the fifty-second quarter of the NBS Semiconductor Technology Program. This Program serves to focus NBS research on improved measurement technology for the use of the semiconductor device community in specifying materials, equipment, and devices in national and international commerce, and in monitoring and controlling device fabrication and assembly. This research leads to carefully evaluated, well-documented test procedures and associated technology which, when applied by the industry, are expected to contribute to higher yields, lower cost, and higher reliability of semiconductor devices and to provide a basis for controlled improvements in fabrication processes and device performance. By providing a common basis for the purchase specifications of government agencies, improved measurement technology also leads to greater economy in government procurement. Financial support of the Program is provided by a variety of Federal agencies. The sponsor of each technical project is identified at the end of each entry in accordance with the following code: 1. The National Bureau of Standards; 2. The Defense Advanced Research Projects Agency; 3. The Division of Electric Energy Systems, Department of Energy; 5. The Defense Nuclear Agency; 6. The C. S. Draper Laboratory; 10. The Naval Weapons Support Center; 11. The Solar Energy Research Institute; 13. The Lewis Research Center, National Aeronautics and Space Administration; and 15. The Naval Ocean Systems Center.

This report is provided to disseminate results rapidly to the semiconductor community. It is not meant to be complete; in particular, references to prior work either at NBS or elsewhere are omitted. The Program is a continuing one; the results and conclusions reported herein are subject to modification and refinement. Further information may be obtained by referring to more formal technical publications or directly from responsible staff members, telephone: (301) 921-listed extension. General information, past issues of progress briefs, and a list of publications may be obtained from the Semiconductor Materials and Processes Division, National Bureau of Standards, Washington, D.C. 20234, telephone: (301) 921-3786.

U.S. DEPT. OF COMM. BIBLIOGRAPHIC DATA SHEET (See Instructions)	1. PUBLICATION OR REPORT NO. NBSIR 81-2230-3	2. Performing Organ. Report No. PB82 135898	3. Publication Date November 1981

4. TITLE AND SUBTITLE

Semiconductor Technology Program - Progress Briefs

5. AUTHOR(S)
K. F. Galloway, R. J. Scace, and E. J. Walters, Editors

342053

6. PERFORMING ORGANIZATION (If joint or other than NBS, see instructions) NATIONAL BUREAU OF STANDARDS DEPARTMENT OF COMMERCE WASHINGTON, D.C. 20234	7. Contract/Grant No.
	8. Type of Report & Period Covered Interim 4/1/81 to 6/30/81

10. SUPPLEMENTARY NOTES

☐ Document describes a computer program; SF-185, FIPS Software Summary, is attached.

11. ABSTRACT (A 200-word or less factual summary of most significant information. If document includes a significant bibliography or literature survey, mention it here)

This report provides information on the current status of NBS work on measurement technology for semiconductor materials, process control, and devices. Emphasis is placed on silicon and silicon-based devices. Highlighted activities include semi-insulating GaAs characterization, an automatic scanning spectroscopic ellipsometer, linewidth measurement and coherence, bandgap narrowing effects in silicon, the evaluation of electrical linewidth uniformity, and arsenic-implanted profiles in silicon. In addition, recent publications and publications in press are listed. The report is not meant to be exhaustive; contacts for obtaining further information are listed.

12. KEY WORDS (Six to twelve entries; alphabetical order; capitalize only proper names; and separate key words by semicolons)

Electronics; integrated circuits; measurement technology; microelectronics; semiconductor devices; semiconductor materials; semiconductor process control; silicon.

13. AVAILABILITY	14. NO. OF PRINTED PAGES
☒ Unlimited ☐ For Official Distribution. Do Not Release to NTIS ☐ Order From Superintendent of Documents, U.S. Government Printing Office, Washington, D.C. 20402.	12
☐ Order From National Technical Information Service (NTIS), Springfield, VA. 22161	15. Price

Bandgap Narrowing Effects in Silicon

The effects of heavy doping on the density of states and the energy bands are important for the interpretation of device behavior. The average shift of the conduction and valence bands due to the interaction of electrons and holes with donor impurities has been calculated by using a partial wave analysis. In order to demonstrate feasibility, or proof of concept, this work was restricted initially to states near the band edge since only the $\ell = 0$ partial wave would be important. The model Yukawa potential was also approximated with a potential due to Bargmann for which the $\ell = 0$ phase shift for the latter potential can, unlike that for the Yukawa potential, be expressed as a function of the wavenumber in closed form. This decreased the computational expense considerably. The success of the above method justified the following improvements. The range of validity in wavenumber was extended by including the partial waves with $\ell = 1$ and $\ell = 2$ as well as $\ell = 0$. The Yukawa potential was also used throughout since numerical solutions for the phase shifts are necessary whenever $\ell > 1$ even for the potential due to Bargmann. An additional refinement has been the self-consistent calculation of the screening length associated with the Yukawa potential by satisfying the Friedel sum rule. The results of this calculation show important differences between this technique and the Fermi-Thomas approach.

The shifts in the energy gap resulting from these calculations are smaller than the shifts measured optically. The difference between the experimental data and these results is due to many body effects, primarily exchange and correlation. In fact, the results of Mahan for these contributions, which are valid at

0 K, when added to these results yield good agreement with the data at 0 K. At room temperature, it is not possible to make such a direct comparison. Good agreement also is obtained between these results for the Fermi energy measured with respect to the conduction band edge and the corresponding optical data. The bandgaps from optical data are much smaller than the bandgaps from electron device experiments. The implication is that other effects, such as variation of the recombination lifetime, should be included in the analysis of the electrical measurements.

An important result of these calculations is that not only is the energy gap narrowed, but the shape of the bands is changed as well. If one were to try to fit parabolic bands to the perturbed bands over a given region necessary for computations, the effective mass of the new parabolic bands would be different from the unperturbed values and would depend upon the extent of the region fitted.

These results have been applied to process modeling by considering the effect of bandgap narrowing on the diffusion coefficients of donor ions at processing temperatures. These coefficients depend strongly on the ratio of the electron density to the intrinsic carrier density. An important question is whether bandgap narrowing effects significantly alter the interpretation of diffusion data as would be implied by the results of other workers for donor and vacancy activity coefficients. The result of applying this model to a sample containing a donor density of 1.0×10^{20} cm^{-3} at 1100°C is a bandgap reduction, $-\Delta E_g$, of 123 meV. However, the ratio of the effective intrinsic carrier density, n_{ie} to the undoped value, n_i, is only 1.15, which is much less than one obtains from the expres-

sion $\exp(-\Delta E_g/2kT)$, i.e., 1.68. The reason for this large difference is that the density of states is highly distorted from its parabolic form. The model described here is very different from previous models and in general yields much smaller values of the ratio n_{ie}/n_i. [Sponsor: 1]

(J. R. Lowney and H. S. Bennett, x3625)

Arsenic-Implanted Profiles in Silicon

Device performance will become more sensitive to the three-dimensional nature of implanted and annealed distribution of the dopants with the trend toward smaller device dimensions for very high speed, very large scale integrated circuits. This may serve as the limiting factor in device performance. The two-dimensional distribution of arsenic implanted into silicon was studied in this work.

The basis of the present understanding of the vertical distribution of ions implanted into an amorphous target is the Winterbon code which is based upon the numerical solution of the Boltzmann equation for the moments of the distribution. Extension of these calculations to two dimensions is nontrivial. However, there are Monte Carlo codes, specifically the TRIM (Transport of Ions into Matter) due to Biersack and Haggmark, which may be used to construct the two-dimensional distribution of ions implanted into amorphous targets. Both of these codes have been used to construct the vertical distribution of arsenic implanted into silicon at 150 keV and yield similar results for the same choice of the ion-atom potential. In addition, these results have been compared with experimental data from SIMS and the three are in good agreement with one another. Further, the TRIM code has been used to construct the two-dimensional distribution of arsenic implants and these results serve as the basis for a physical understanding of the experimental results discussed here.

In addition, the predictions of the SUPREM-II code for process modeling supplemented with the more recent understanding of the arsenic diffusion process have been employed in the evaluation of the results of annealing studies of arsenic-implanted regions.

In the experimental study, specially prepared specimens fabricated at Hughes Research Laboratories , were employed. Specifically, boron-doped silicon wafers were prepared with a grating pattern structure on the surface. This pattern served to mask out the incident arsenic ions during the implantation process allowing the arsenic to enter only the silicon lattice in parallel stripe regions. The wafers were annealed under various time-temperature conditions in order to ascertain the effects of the anneal cycle on the distribution of the arsenic atoms due to both the original implantation process and the anneal-induced redistribution.

After the patterned wafers had been implanted and annealed, the photoresist and aluminum stripe pattern were removed and the wafers were cleaned with standard peroxide solutions. Finally, the wafers were cleaved perpendicular to the grating fingers. Two anneal temperatures were used in the study: 600°C, to remove the initial implant damage and to activate the arsenic with minimal redistribution; and 1000°C, to determine the effect of the anneal-induced diffusion on the final junction location (both vertical and lateral). To determine the junction location, both etch and EBIC (Electron Beam Induced Current) techniques were used. It is important to note that this is the first time that these techniques have been used in the depth scale required for VLSI and VHSIC structure investigation.

The etch technique, even though there were some problems with the application of "wet chemistry" to submicrometer dimensions, showed that the 600°C annealed arsenic had no appreciable signs of lateral channeling, while the 1000°C

annealed arsenic had significant signs of lateral diffusion.

The EBIC data are in substantial agreement with this conclusion. In principle, the EBIC data should be able to provide not only the location of the vertical and lateral junction but also the distribution of activated dopants. However, this requires the numerical solution of the semiconductor transport equations in the presence of electron-hole pair generation due to the electron beam.

The above observations are in substantive agreement with the results of the two-dimensional Monte Carlo (TRIM) calculations in that they show very little lateral spreading of arsenic when implanted into silicon. This can be understood on the grounds that arsenic is more massive than silicon and is unlikely to be deflected in the lateral direction by the silicon atoms. On the other hand, dopants lighter than silicon, boron, for example, might show appreciable lateral spreading. The diffusion predictions of the augmented SUPREM-II code agrees well with the vertical junction location. [Sponsor: 15]

(J. Albers, J. R. Ehrstein, D. R. Myers,* and P. Roitman, x3625)

Electrical Linewidth Uniformity Evaluation

An electrical measurement method using the cross-bridge test structure to evaluate linewidth variation associated with integrated circuit lithography has been developed. Arrays of identical cross-bridge resistors were patterned in an aluminum layer on a silicon wafer using a single photomask. Electrical test results from these structures were used to measure the uniformity of the linewidth across a wafer and across a chip. The data were analyzed to evaluate the linewidth uniformity of a step-and-repeat system. Techniques were developed to identify and remove systematic linewidth variations introduced by other
_____
*Present address: Sandia Laboratories, Albuquerque, New Mexico.

aspects of the photolithography process and to determine the precision of the measurement.

Analysis was made from data of test chip NBS-23. NBS-23 is a test chip consisting of an 20 by 12 array of identical cross bridges with design linewidths of 6 μm. The array fits within a square 250 mil (6.35 mm) on a side and is repeated across the photomask. A wafer is then fabricated by delineating the cross bridges (using contact printing and wet chemical etching) in an 800-nm thick aluminum film evaporated on an oxidized silicon wafer. The automated dc test system used to make the measurements consists of a minicomputer-controlled wafer prober, scanners, digital current source, and digital voltmeter. Approximately 3 s were required to measure each cross bridge.

In order to determine linewidth uniformity with this test chip, it is important to know the measurement precision which determines the achievable resolution. Linewidth measurement precision is limited by the test system and the test structure. The precision of the test system was determined by repeated measurements of the electrical linewidth on the same cross bridge and a computation of the sample standard deviation. The precision was found to be 0.002 μm (1σ) for sixty measurements. To determine the usable precision of the test structure, a sample of the measurement data was analyzed. Test results from one row of cross bridges across the wafer representing seven adjacent test chips, each chip containing 20 cross bridges, are shown in the accompanying figure. Three types of variations can be seen: a random variation, a systematic intrachip variation, and a systematic intrawafer variation. The magnitude of the random variation determines the achievable measurement precision of the test structure. To estimate the magnitude of the random variations correctly, the systematic variations in the data must be removed. This was accomplished by fitting the data to a fourth-degree poly-

5
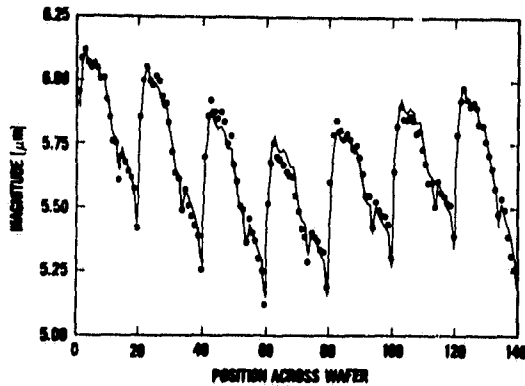
NBS-23 data of linewidth measurements from one row across the center of the wafer (●) and the fitted function.

nomial which estimated the intrawafer and intrachip variation. The result of this fit can also be seen in the figure in the form of the connected line which is the sum of the two estimated mathematical functions. The residual standard deviation after subtracting the estimated functions from the original data is 0.03 μm (1σ).

Electrical linewidth measurements with the cross-bridge test structures fabricated on silicon wafers can resolve variations in linewidth to a precision of 0.03 μm (1σ). This level of precision allows this technique to be used as a valuable tool for evaluating the performance of lithography systems capable of submicrometer resolution. [Sponsor: 1]   (D. Yen and L. W. Linholm, x3541)

Linewidth Measurement and Coherence

Earlier work on optical methods for linewidth measurement for IC photomasks and wafers led to the development of the method of coherent edge detection. In the coherent case, the optical intensity or threshold corresponding to edge location was given by

$$T_C = 0.25\left(I_O + I_M + 2\sqrt{I_O I_M}\cos\phi_O\right),$$

where I_O and I_M are the reflectances (or transmittances) of the etched layer

and substrate, respectively, and ϕ_O is the optical phase difference at the line edge which occurs on reflectance (or transmittance). It has now been shown that this equation is a special case of a more general expression for determining the threshold corresponding to the line edge location which can be applied to any state of partial coherence and allows the inclusion of known optical aberrations such as defocus. In the more general case, the threshold T_{PC} is defined as the ratio of the optical intensity in the image at the line edge to the reflected (or transmitted) optical intensity from the substrate, i.e., using a Fourier series representation of the image,

$$T_{PC} = \frac{\displaystyle\sum_{n=-\infty}^{\infty} b_n \cos\frac{\pi n W}{P}}{\displaystyle\sum_{n=-\infty}^{\infty} b_n},$$

where the linewidth is W and the period P can be chosen arbitrarily large to describe isolated lines. For partially coherent illumination, the Fourier coefficients b_n are given by

$$b_n = A_n A_O^* \; T\left(\frac{n}{P},\, 0\right)$$

$$+ \sum_{n'=1}^{\infty} \left\{ A_{n+n'} A_{n'}^* T\left(\frac{n+n'}{P},\, \frac{n'}{P}\right) \right.$$

$$\left. + A_{n-n'} A_{-n'}^* T\left(\frac{n-n'}{P},\, \frac{-n'}{P}\right) \right\},$$

where

$$A_O = \frac{1}{2}\left\{1 + \sqrt{I_O/I_M}\exp(i\phi_O)\right\},$$

$$A_n = \frac{1}{2}\left\{1 - \sqrt{I_O/I_M}\exp(i\phi_O)\right\}\frac{\sin(\pi n/2)}{(\pi n/2)}.$$

This equation assumes well-resolved lines where, for convenience only, the linewidth has been taken to be half the

6

period $(W/P = 1/2)$. The function T is called the transmission cross coefficient and characterizes the 2-D (two-dimensional) optical system including the partial coherence in the illumination. For a 1-D (one-dimensional) line object

$$T(\xi_1, \xi_2) = \int_{-\infty}^{\infty} \int_{-\infty}^{\infty} A(\xi'', \eta'') F(\xi_1 + \xi'', \eta'')$$

$$\times F^*(\xi_2 + \xi'', \eta'') \, d\xi'' \, d\eta'' \, ,$$

where $A(\xi'', \eta'')$ is the 2-D intensity distribution in the condenser aperture (wide-field Kohler or critical illumination assumed). The function A is sometimes called the effective source (assumed to be incoherent; i.e., the coherence interval is small compared to the effective source size). F is the pupil function of the optical system in normalized coordinates.

Even with spatially incoherent sources, a finite degree of partial coherence is generated with propagation of light through the optical system due to the finite dimensions of the source and apertures. For wide-field microscope illumination, and either critical or Kohler illumination, the degree of coherence (spatial) is determined by the ratio of condenser to objective numerical aperture, frequently called the coherence parameter R. The transmission cross coefficients represent a correlation of these aperture functions. In the first figure, T_{PC} is plotted for matched condenser and objective numerical apertures. Imaging with matched apertures was once thought to be "incoherent." However, the obvious sensitivity of the edge detection threshold to the optical phase difference at the line edge is further proof that this is not the case, and the matched aperture condition instead represents an intermediate case of partially coherent imaging. The 33% threshold used for edge detection with matched apertures was first noted by Charman. As may be seen in the figure, a 33% threshold applies only to
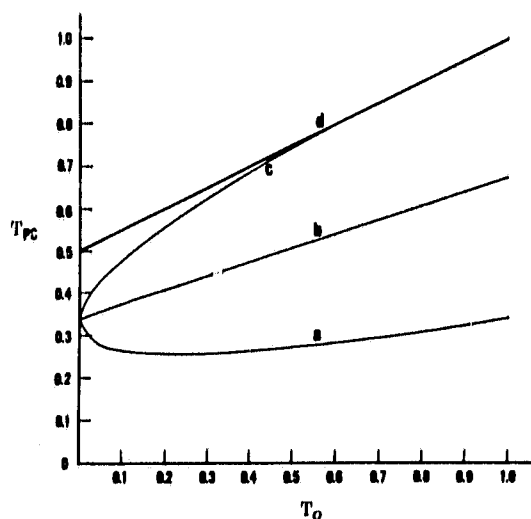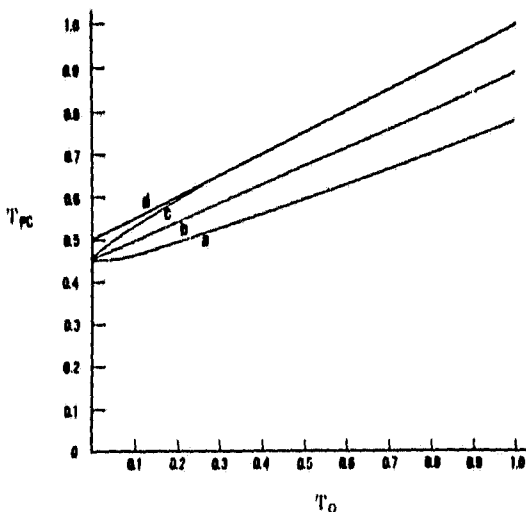

Threshold T_{PC} corresponding to edge location for coherence parameter $R = 1$ as a function of T_0 (I_0/I_M). Curve-to-curve parameter is optical phase difference ϕ_0: a) π, b) $\pi/2$, c) 0. The 50% incoherent edge detection threshold is shown (curve d) for comparison.

high contrast $(I_0/I_M = 0)$ line objects where the optical phase difference may be ignored.

Although it is not possible to achieve effectively incoherent illumination in high resolution wide-field microscopy (with a dry objective, 0.9 N.A., R values appreciably greater than 1.0 are not possible), it is of interest to many microscopists to determine the value of R required for effectively incoherent illumination. The second figure (next page) shows the threshold variation for $R = 2$. This figure indicates that a phase difference of π, which should not be visible in incoherent illumination, for $R = 2$ would image as a dark line with a modulation of 12% and thus would be visible to the eye as well as to a photodetector. Therefore, effective incoherence for sharp edges requires an R value greater than 2.

The formalism of the transmission cross-coefficients allows the inclusion of optical aberrations such as defocus in

7

Threshold T_{PC} corresponding to edge location for coherence parameter $R = 2$ as a function of T_O (I_O/I_M). Curve-to-curve parameter is optical phase difference ϕ_O: a) π, b) $\pi/2$, c) 0. The 50% incoherent edge detection threshold is shown (curve d) for comparison.
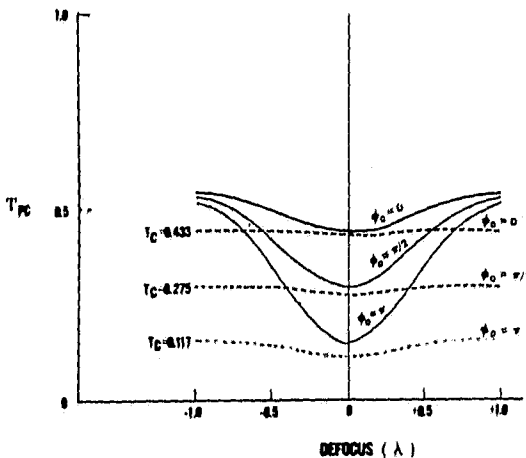

Variation of T_{PC} with defocus parameter a_2 for $T_O = 0.1$, for different R values: dashed lines $R = 1/5$, solid lines $R = 2/3$. The coherent edge detection threshold T_C is indicated in each case and is equivalent to the value of T_{PC} for zero defocus and $R = 1/5$.

terms of the pupil function of the imaging optics. For defocus, the pupil function becomes

$$F_{defocus}(\rho) = \exp\left(ika_2\rho^2\right) \quad \rho = \left(\xi^2 + \eta^2\right)$$

where a_2 indicates the amount of defocus in waves (units of wavelength) and k is the wave number. The third figure shows the variation of the edge detection threshold with focus for selected values of T_O and ϕ_O. Note that with increased coherence the edge detection threshold is less sensitive to defocus and thus measurement precision improves. [Sponsor: 1]   (D. Nyyssonen, x3621)

Semi-Insulating GaAs Characterization

A measurement technique for characterizing electrically active traps in semi-insulating (SI) semiconductors has shown potential for further development. The technique, termed photoinduced resistance-deep level transient spectroscopy (PR-DLTS), permits electrical characterization of high resistivity semiconductors such as SI GaAs, for which many conventional electrical techniques are inadequate. In PR-DLTS, monochromatic light is used to create excess free carriers in the material which are then trapped by the deep levels. After the light is extinguished, the excess free carriers recombine, and there occurs a transient change in the specimen conductivity as the carriers, trapped at the deep levels, are emitted and the system returns to thermodynamic equilibrium. The rate at which the trapped carriers are emitted is a characteristic function of the particular trap involved and the temperature. This emission rate is measured as a function of temperature resulting in a signature of the particular trapping center.

The transient conductance is measured in an impedance bridge at 10 MHz and signal processing is performed as in conventional DLTS. In the PR-DLTS measurement, however, specimen capacitance is fixed by a parallel plate test structure with the SI GaAs assuming the role of a

8
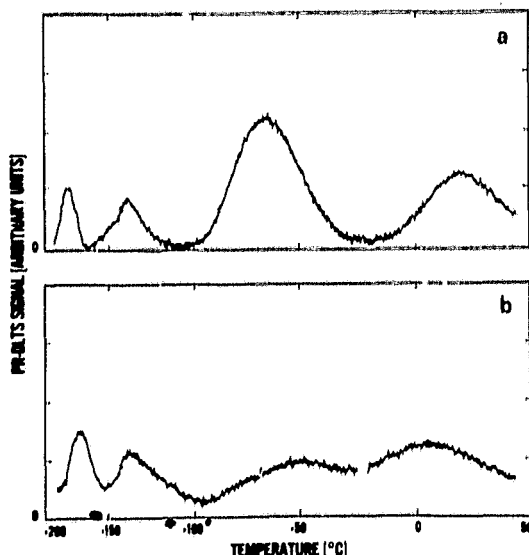
Photoinduced resistance-DLTS measurement of semi-insulating GaAs for LEC-grown material (a) and HB-grown material (b).

dielectric. Light illuminates the SI GaAs surface through spaces in an aluminum grid contact. By phase-sensitive rf detection techniques the resistive portion of the transient is monitored as opposed to the capacitive portion in conventional DLTS. Results to date show that the method is capable of discriminating between variously grown specimens of SI GaAs as displayed in the accompanying figure. PR-DLTS spectra are presented for two specimens of SI GaAs grown by the same manufacturer, but by two different techniques: liquid encapsulated Czochralski (LEC) and horizontal Bridgman (HB). As can be seen, four peaks are evident in both the LEC and HB spectra, each peak corresponding to a specific deep level. Interpretation of these data in terms of particular impurities, densities, and energy levels has not yet been established.

PR-DLTS shows promise as a tool to electrically characterize device starting material as well as to correlate material properties with device performance parameters. It offers the advantage, over other electrical and photoelectronic methods, of noncritical contacts. The system is also readily constructed by simple modifications of a conventional DLTS system.

Recent findings have shown the PR-DLTS spectra to be a function of light excitation wavelength, intensity, and duration. These effects are presently being examined. In addition, experiments are planned to correlate the PR-DLTS data with other electrical, optical, and physical measurement techniques as well as to interpret the results in terms of specific deep level states. [Sponsor: 1]   (A. C. Seabaugh, x3625)

Automatic Spectroscopic Ellipsometer

A new scanning automatic spectroscopic ellipsometer is being built in the Semiconductor Materials and Processes Division. This ellipsometer will be a variable angle of incidence instrument that can be run in either an automated principal angle of incidence mode, rotating analyzer mode, or conventional automatic null mode. Each method has its own advantages depending upon the user's needs, but an important feature will be the ability to intercompare these methods. The mechanical design is one based on rotating goniometers powered by stepping motors as used, for example, in x-ray diffraction instruments. The goniometers have very high accuracy and precision required for this ellipsometer. The light sources will be a standard HeNe laser (632.8-nm wavelength) and also a HeCd (441.6-nm wavelength) laser. In addition, a prism-grating monochromator (186- to 2650-nm wavelength, corresponding to 6.7 to 0.47 eV) will be used for spectroscopic studies. The optics will include standard ellipsometric polarizers and compensators. The automation will be carried out by the use of a computer interfaced to address the components of the instrument, which include the stepping motor controlled goniometers and a photomultiplier or solid-state light detector.

9

Communications from readers having an interest in precise ellipsometric measurements are welcomed. [Sponsor: 1] (G. A. Candela and D. Horowitz, x3625)

Erratum in ASTM F 723-81

A printing error exists in ASTM F 723-81 for conversion between resistivity and dopant density. This standard practice is based on NBS data. The correct equation to convert resistivity to dopant density for boron-doped silicon is:

$$N = \frac{1.330 \times 10^{16}}{\rho} + \frac{1.0824 \times 10^{17}}{\rho\left(1 + (54.56 \ \rho)^{1.105}\right)}$$

[Sponsors: 1,2] (J. R. Ehrstein, x3625)

Recent Publications . . .

Wilson, C. L., and Blue, J. L., Semiconductor Device Simulation, *Proc. Conf. Elliptic Problem Solvers,* Sante Fe, New Mexico, June 30–July 2, 1980, pp. 435–439 (Academic Press, New York).

Bullis, W. M., and Scace, R. I., The Department of Commerce and the Role of Government Standards, Chapter in *VLSI Electronics, Microstructure Science,* Vol. 1, Norman G. Einspruch, Ed. (Academic Press, New York, 1981) (same as NBSIR 80-2057).

Myers, D. R., Wilson, R. G., and Comas, J., Effect of Silicon Dioxide Surface-Layer Thickness on Boron Profiles for Directly Aligned Implants Into (110) Silicon, *J. Appl. Phys.* 52, 3357–3359 (May 1981).

Buehler, M. G., and Perloff, D. S., Microelectronic Test Chips and Associated Parametric Testers: Present and Future, *Semiconductor Silicon/1981,* H. R. Huff, R. J. Kriegler, and Y. Takeishi, Eds., pp. 859–867 (ECS, Pennington, New Jersey, May 1981).

Linholm, L. W., Mattis, R. L., Frisch, R. C., and Reeves, C. P., Characterizing and Analyzing Critical Integrated Circuit Process Parameters, *Semiconductor Silicon/1981,* H. R. Huff, R. J. Kriegler, and Y. Takeishi, Eds., pp. 906–920 (ECS, Pennington, New Jersey, May 1981).

Berning, D. W., and Blackburn, D. L.,

The Effect of Magnetic Package Leads on the Measurement of Thermal Resistance of Semiconductor Devices, *IEEE Trans. Electron Devices* ED-28, 609–611 (May 1981).

Larrabee, R. D., Thurber, W. R., and Bullis, W. M., Electrical Parameters of Extrinsic Silicon, *Circuits Manufacturing* 21 (5), 92–100 (May 1981).

Buehler, M. G., and Linholm, L. W., Toward a Standard Test Chip Methodology for Reliable, Custom Integrated Circuits, *Proc. 1981 Custom Integrated Circuits Conf.,* Rochester, New York, May 11–13, 1981, pp. 142–146.

Peckerar, M. C., and Galloway, K. F., Informal Survey of Federal Government Microelectronics Processing Facilities, *Proc. 4th Biennial University/Government/Industry Microelectronics Symp.,* Mississippi State University, May 1981, pp. III-24 – III-30.

Forman, R. A., Myers, D. R., and Bell, M. I., Comments on "Raman Scattering from Boron-Implanted Laser Annealed Silicon," *J. Appl. Phys.* 52, 4337–4339 (June 1981).

Lowney, J. R., Kahn, A. H., Blue, J. L., and Wilson, C. L., Disappearance of Impurity Levels in Silicon and Germanium Due to Screening, *J. Appl. Phys.* 52, 4075–4080 (June 1981).

Ruthberg, S., Graphical Solution for the Back Pressurization Method of Hermetic Test, *IEEE Trans. Components, Hybrids, and Manufacturing Tech.* CHMT-4, 217–224 (June 1981).

Publications in Press . . .

Albers, J., Probe-Spacing Experiment Simulation and the Relation Between Spreading Resistance and Sheet Resistance, *J. Electrochem. Soc.*

Baghdadi, A., and Forman, R. A., Tertiary Interferograms in Fourier Transform Spectroscopy, *Appl. Spectrosc.*

Bennett, H. S., Upper Limits for the Number of Bound States Associated with the Yukawa Potential, *NBS J. Res.*

Bennett, H. S., and Lowney, J. R., Effect of Donor Impurities on the Density of States Near the Band Edge in Silicon, *J. Appl. Phys.*

Berning, D. W., Use of Vacuum Tubes in Test Instrumentation for Measuring Characteristics of Fast High-Voltage Semiconductor Devices, *IEEE Trans.*

Instrum. & Measurement.

Blackburn, D. L., Robbins, T. C., and Galloway, K. F., VDMOS Power Transistor Drain-Source Resistance Radiation Dependence, *IEEE Trans. Nucl. Sci.*

Buehler, M. G., and Linholm, L. W., The Role of Test Chips in Coordinating Logic Design and Layout Aids for VLSI, *Proc. 2nd Cal. Tech. Conf. on VLSI,* Pasadena, California, January 1981.

Bullis, W. M., Trends in Integrated Circuit Metrology, *EDN Magazine.*

Bullis, W. M., and Nyyssonen, D., Optical Linewidth Measurements on Photomasks and Wafers, Chapter in *VLSI Electronics, Microstructure Science,* Vol. 3, Norman G. Einspruch, Ed. (Academic Press, New York).

Candela, G. A., Galloway, K. F., Liu, Y. M., and Fine, J., Measurements of the Interlayer Between Al and SiO_2 Using Ellipsometric, Capacitance-Voltage, and Auger Electron Spectroscopy Techniques, *Thin Solid Films.*

Carver, G. P., Development of Test Structures for Characterization of the Fabrication and Performance of Radiation-Hardened Charge-Coupled Device (CCD) Imagers: Annual Report, May 15, 1980 to May 14, 1981, NBSIR 81-2319.

Harman, G. G., The Use of Acoustic Emission as a Test Method for Microelectronic Interconnections and Joints, *Proc. 2nd Internat. Conf. Loten und Schweissen in Der Elektronik.*

Larrabee, R.D., Phillips, W. E., and Thurber, W. R., Measurement Techniques for High Power Semiconductor Materials and Devices: Annual Report, October 1, 1979 to September 30, 1980, NBSIR 81-2325.

Leedy, T. F., Temperature Dependence of Transient Electron Radiation Upset in TTL Circuits, *IEEE Trans. Nucl Sci.*

*Li, S. S., Conductivity Mobility, Hall Mobility, and Resistivity in *p*-Type Silicon, NBS-GCR-81-334.

*Lin, J. F., Li, S. S., Linares, L. C., and Teng, K. W., Theoretical Analysis of Hall Factor and Hall Mobility in *p*-Type Silicon, *Solid-State Electronics.*

Linholm, L. W., *Semiconductor Measurement Technology:* The Design, Testing, and Analysis of a Comprehensive Test Pattern for Measuring CMOS/SOS Process Performance and Control, NBS Spec. Publ. 400-66.

Lowney, J. R., and Bennett, H. S., Effect of Donor Impurities on the Conduction and Valence Bands of Silicon, *J. Appl. Phys.*

*McCarthy, D., Acevedo, J., and Herman, D., Advanced Planar Silicon Test Structures, NBS-GCR-81-327.

Mitchell, M. A., Linholm, L. W., Russell, T. J., and Carver, G. P., Electrical Test Structures for Characterization and Control of Microelectronics Processing, *Proc. Microelectronic Measurements Technology Workshop,* San Jose, California, March 23, 1981.

Phillips, W. E., Improved Thermometry for Deep-Level Measurements, *J. Physics E.*

Schafft, H. A., Measurements for Commercial Photovoltaics, - A Status Report, SERI.

*Schwarz, S. A., Helms, C. R., Spicer, W. E., and Taylor, N. J., *Semiconductor Measurement Technology:* The Capabilities and Limitations of Auger Sputter Profiling for Studies of Semiconductors, NBS Spec. Publ. 400-67.

Wilson, C. L., and Blue, J. L., Two-Dimensional Finite Element Charge-Sheet Model of a Short-Channel MOS Transistor, *Solid-State Electronics.*

*Wilson, R. G., and Jamba, D. M., *Semiconductor Measurement Technology:* Differential Capacitance-Voltage Profiling of Schottky Barrier Diodes for Measuring Implanted Depth Distributions in Silicon, NBS Spec. Publ. 400-71.

*Reports of contract research.